

# Subleading EW corrections and spin-correlation effects in $t\bar{t}W$ multi-lepton signatures

Rikkert Frederix<sup>\*1</sup> and Ioannis Tsinikos<sup>†2</sup>

<sup>1,2</sup>Theoretical Particle Physics, Department of Astronomy and Theoretical Physics, Lund University, Sölvegatan 14A, SE-223 62 Lund, Sweden

April 22, 2020

## Abstract

Recently a slight tension between data and predictions has been reported in  $t\bar{t}W$  production by both the CMS and ATLAS collaborations. We revisit the theoretical predictions for this process, focussing on the following two effects. We disentangle various effects that lead to asymmetries among the leptonic decay products of the (anti-)top quarks and  $W$  bosons, for which we find that the spin correlations in the top-quark pair are the dominant source. We also discuss the impact of the large, formally subleading, electroweak corrections to  $t\bar{t}W$  production at the LHC. We find that this effect changes the  $t\bar{t}W$  cross section significantly in the signature phase-space regions, and should therefore be included differentially in the theory to data comparisons.

## 1 Introduction

With the 13 TeV LHC run, both ATLAS and CMS collaborations have measured the  $t\bar{t}V$  ( $V = Z, W$ ) cross sections. These processes are studied either independently [1, 2] or as irreducible backgrounds to  $t\bar{t}H$  (multilepton) searches [3, 4]. In both cases a slight tension between theoretical predictions and data is observed for  $t\bar{t}W$  production, with the data suggesting a somewhat larger cross section than Standard Model predictions. This slight tension between Standard Model predictions and data warrants further study of this process from both the experimental and the theoretical sides.

At the production level the  $t\bar{t}W$  process has recently been studied in detail at the complete-NLO accuracy [5]. In this work it was pointed out that the subleading EW corrections result in a  $\sim 10\%$  increase of the total cross section. This large contribution is due to the opening of  $tW \rightarrow tW$  scattering diagrams. The complete-NLO calculation has been matched to soft (threshold) gluon resummation, resulting in the most-accurate predictions for the  $t\bar{t}W$  production at the LHC to date [6, 7]. Both these works have shown that  $t\bar{t}W$ , in contrast to  $t\bar{t}Z$  and  $t\bar{t}H$ , does not become less sensitive to the scale choices

---

<sup>\*</sup>rikkert.frederix@thep.lu.se

<sup>†</sup>ioannis.tsinikos@thep.lu.se

even when including the resummation at NNLL accuracy. In other words, including the all-order soft-gluon resummation does not significantly decrease the theoretical uncertainties. This can predominantly be attributed to the absence of gluon-induced channels at LO; the latter only appear at higher orders and give sizeable contributions to the cross section. Since they do not contribute at LO they are not considered in the resummation frameworks of refs. [6, 7]. Incidentally, since the  $gg$  channels only open at NNLO accuracy there is a large  $t\bar{t}$  asymmetry of  $\sim 3\%$  in  $t\bar{t}W$  production [6, 8, 9].

At the decay level this accuracy cannot be maintained due to the complexity of the calculation. It is shown in ref. [8] that the presence of the  $W$  boson polarises the initial quark-line and in turn the final  $t\bar{t}$  pair. The emerged lepton asymmetry is of  $\sim 13\%$  at NLO in QCD and has consequences on the final lepton pseudo-rapidity distributions. Therefore it affects the fiducial region of the final multi-lepton signatures depending on the applied cuts. Furthermore the subleading EW  $tW \rightarrow tW$  scattering contributions are governed by different kinematics and as a result a non-flat effect is expected in the fiducial region.

Since the largest tension for  $t\bar{t}W$  is found when it enters as the main background in the  $t\bar{t}H$  multi-lepton analyses, these multi-lepton signatures is what we focus on in this work. We study all effects that lead to lepton asymmetries in detail. We further study contributions that have not been yet taken under consideration in the fiducial region: for the first time, we include the subleading EW corrections in a consistent matching to the parton shower. The latter allows us to investigate the effects from these large corrections differentially in the fiducial region relevant to the  $t\bar{t}H$  multi-lepton signatures.

The structure of this paper is the following: in section 2 we discuss the input parameters, describe the framework of the calculation and we define the experimental fiducial region under study. In section 3 we discuss the main subleading EW and spin-correlation effects on differential distributions and their impact on measurements. We present our conclusions in section 4.

## 2 Input parameters and calculation setup

We consider the NLO corrections to both  $pp \rightarrow t\bar{t}W^+$  and  $pp \rightarrow t\bar{t}W^-$  production in the fiducial region following the ATLAS analysis of ref. [3]. The calculation is performed within the MadGraph5\_aMC@NLO [10] framework including the automation of the EW calculations [11]. In accordance with the notation of [5] we define for any observable the QCD and subleading EW ( $\text{EW}_{\text{sub}}$ ) perturbative orders as following:

$$\begin{aligned}\Sigma_{\text{QCD}} &= \alpha_s^2 \alpha \Sigma_{3,0}^{t\bar{t}W} + \alpha_s^3 \alpha \Sigma_{4,0}^{t\bar{t}W} \\ &= \Sigma_{\text{LO}_1} + \Sigma_{\text{NLO}_1} \\ \Sigma_{\text{EW}_{\text{sub}}} &= \alpha^3 \Sigma_{3,2}^{t\bar{t}W} + \alpha_s \alpha^3 \Sigma_{4,2}^{t\bar{t}W} \\ &= \Sigma_{\text{LO}_3} + \Sigma_{\text{NLO}_3}.\end{aligned}\tag{2.1}$$

We perform the calculation in the 5 Flavour Scheme, setting the factorisation and renormalisation scales to  $\mu = \frac{H_T}{2}$  and using the NLO PDF4LHC PDF sets, with associated value for the strong coupling. As input parameters we use

$$\begin{aligned}m_t &= 173.34 \text{ GeV}, \quad m_Z = 91.1876 \text{ GeV} \\ a_{EW} &= 132.232, \quad G_f = 1.16639 \times 10^{-5}.\end{aligned}\tag{2.2}$$

The top quarks are decayed to  $b$  quarks and  $W$ -bosons with a branching ratio of 100%. The  $W$  bosons are decayed inclusively, i.e. both the prompt  $W$  bosons and the ones induced by the top quark decays are allowed to decay to quarks and leptons. Unless stated otherwise, all these decays are realised within the MadSpin framework [12] in order to fully keep the (LO) spin correlations.

We match the calculation to the parton shower using the PYTHIA8 framework [13] in the default tune, using MadGraph5\_aMC@NLO's build-in MC@NLO matching technique [14, 15]. The reason that the  $\text{EW}_{\text{sub}}$  contribution can be included in the matching to the parton shower is that the perturbative order  $\alpha_s\alpha^2$  (the  $\text{LO}_2$  in the notation of ref. [5]) is exactly zero for this process. As a result the  $\alpha_s\alpha^3$  order can be considered as pure QCD corrections to the  $\alpha^3$  one<sup>1</sup>.

In order to understand the spin-related and the subleading EW effects, before applying any particle selection or cuts, we define the inclusive (no cuts) signature. Furthermore, once specified, we select only events for which the top-quark pair decays to a muon pair and the associated  $W$  boson to an electron(positron), using MC-truth. This is done only in order to pin down the origin of various effects and for our final results the decays are inclusive. For the signal-region definitions we start with the selection and the cuts, for which we follow the experimental analysis of [3]. We identify the particles as following:

$$\begin{aligned} \text{Electrons : } & p_T(e) \geq 10 \text{ GeV} , |\eta(e)| \leq 2.47 \text{ (2 for tight)} \\ \text{Muons : } & p_T(\mu) \geq 10 \text{ GeV} , |\eta(\mu)| \leq 2.5 \text{ (same for tight)} \\ \text{jets : } & k_T = -1 , R = 0.4 , p_T(j) \geq 25 \text{ GeV} , |\eta(j)| \leq 2.5 . \end{aligned} \quad (2.3)$$

The  $\tau$  leptons are allowed to decay within the shower and we identify the hadronic  $\tau_h$ . We reject the jets that have  $\Delta R(j, e) \leq 0.3$  or  $\Delta R(j, \tau_h) \leq 0.3$ . Furthermore we discard the muons that lie within  $\Delta R(j, \mu) \leq 0.4$ .

With this particle selection we define the two following signatures: the same sign dilepton ( $2\text{ss}\ell$ ) and the three lepton ( $3\ell$ ) channels. In both cases we require at least two jets and at least one b-tagged jet and zero hadronic  $\tau_h$ 's. For the  $2\text{ss}\ell$  signature we require exactly two tight same sign leptons with  $p_T(\ell) \geq 20$  GeV. Furthermore for the same flavor (SF) pairs we apply the  $m(\ell\ell) \geq 12$  GeV condition. For the  $3\ell$  signature we ask exactly three leptons, two tight same sign (SS) with  $p_T(\ell) \geq 15$  GeV and one opposite sign (OS) with  $p_T(\ell) \geq 10$  GeV. For the SFOS pairs we ask  $m(\ell^+\ell^-) \geq 12$  GeV,  $|m(\ell^+\ell^-) - m_Z| \geq 10$  GeV and for the 3-lepton system  $|m(\ell\ell\ell) - m_Z| \geq 10$  GeV.

In PYTHIA8 we include hadronisation, the QED shower (we include the photons in the jets) and the multiparton interactions (underlying event). However, we do not consider any misidentification or identification inefficiencies for the jets or the leptons.

### 3 Results

Having defined the selection criteria for the particles and the events we proceed now by pointing out the importance of the spin correlations and thereafter showing the effect of the  $\text{EW}_{\text{sub}}$  contributions. In particular, we focus on the jet-multiplicity cross sections, since that is shown by the ATLAS collaboration in ref. [3] (both with prefit and postfit signal+background contributions). However, since the data has not been unfolded, we cannot directly compare to it. On the other hand, we can study this distribution at the

---

<sup>1</sup>What are usually called the EW-corrections, i.e. the  $\alpha_s^2\alpha^2$  perturbative order (a.k.a.  $\text{NLO}_2$ ), are not included here. These EW corrections change the cross section by about  $\sim$ -4% [11, 16].

theoretical level to see firstly whether and how it is shaped by the spin correlations and secondly if the  $\text{EW}_{\text{sub}}$  effects considered in this work might have a significant influence on the ATLAS analysis.

### 3.1 Asymmetries

The effects described in the present section are already included in the modern MC simulations. Nevertheless, they are never disentangled in such detail in order to scrutinise their impact and understand their contribution to the final signatures. Indeed, the asymmetries in the lepton decay products of the  $t\bar{t}W^+$  and  $t\bar{t}W^-$  can be attributed to separate origins, which are depicted in figs. 1 and 2 and described in what follows.

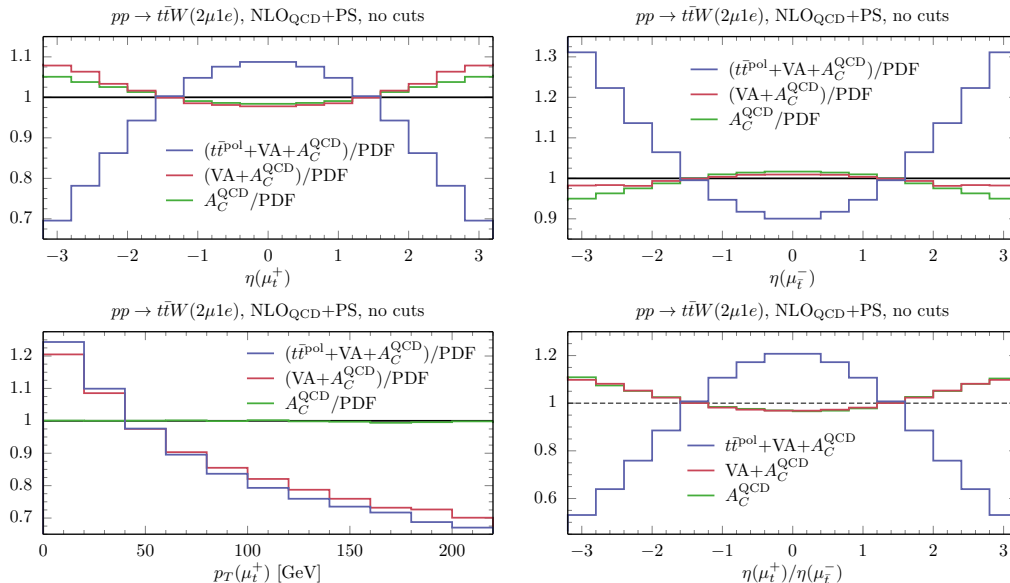


Figure 1: Origin of asymmetries in top pair decay products. The muons in these plots exclusively originate from the top-quark pair.

For these plots, in order to track the origin of the leptons, we have selected the events where the top quark pair decays to muons and the associated  $W^-$  ( $W^+$ ) to electrons (positrons). Furthermore we restrict the analysis only to the QCD shower within PYTHIA8 without applying any cuts or selections. We denote the origin of each lepton with a subscript. In fig. 1 we show the various effects on the decay products of the top pair, whereas in fig. 2 of the associated  $W$  boson. We now separate these effects on the lepton asymmetries:

- The  $t\bar{t}W^+$  production is induced predominately by the  $u\bar{d} + c\bar{s}$  luminosity, while  $t\bar{t}W^-$  one mostly by  $\bar{u}d + \bar{c}s$ . This results in the total cross section for top pairs associated with the positively charged vector boson to be about a factor two larger than the negatively charged vector boson. Moreover,  $t\bar{t}W^+$  typically probes larger Björken  $x$  values than  $t\bar{t}W^-$  resulting, on average, in harder and more forward leptons in the former as compared to the latter. This effect in figs. 1 and 2 is defined as ‘PDF’ and it affects both the top pair and the  $W$  associated decay products. All the other effects are added on top of this. Since in fig. 1 there is no distinction made for muons coming from  $t\bar{t}W^+$  versus muons coming from  $t\bar{t}W^-$ , there is no PDF effect visible here. On the other hand, for the electron/positron coming from the

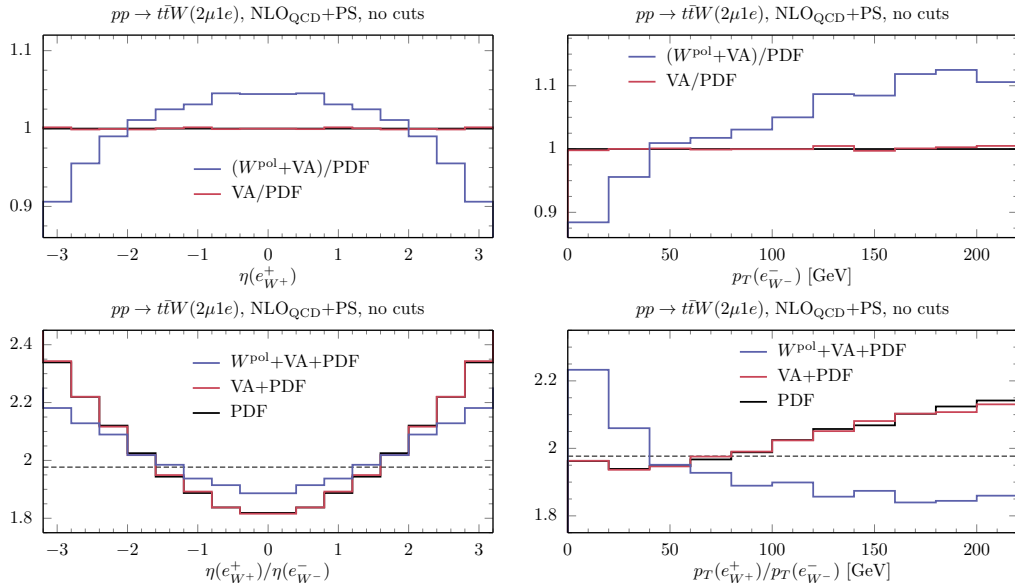


Figure 2: Origin of asymmetries in  $W$  associated decay products. The electrons(positrons) in these plots originate exclusively from the  $W^-(W^+)$  associated boson.

associated  $W$ -boson decay this distinction is made, and therefore the PDF effect is clearly visible in the lower two plots of fig. 2, with the positron from the  $t\bar{t}W^+$  process being at larger rapidities and harder than the electron from the  $t\bar{t}W^-$  process.

- The second cause for differences between the leptonic decay products is due to the Central-Peripheral asymmetry in the top pairs [17–21]. This effect only enters at NLO in QCD, and was first studied for top pair production at the Tevatron, where it showed as a charge asymmetry [22–25]. Compared to  $pp \rightarrow t\bar{t}$  production, requiring the associated  $W$ -boson increases the asymmetry [8]. In fig. 1 this is denoted as ‘ $A_C^{\text{QCD}}$ ’. It results in about 3-5% differences in the pseudo-rapidity of the lepton coming from the top decay versus the one coming from the anti-top decay (pseudo-rapidity insets in fig. 1). It has a negligible effect on the corresponding  $p_T$  distributions (fig. 1).
- The third effect that could lead to asymmetries among the leptonic  $W$ -boson decays is the  $V - A$  structure of the  $W$ -boson couplings. This is denoted in figs. 1 and 2 as ‘VA’ effects. While these effects are not there for the decays of the associated  $W$ -boson (fig. 2), the  $V - A$  coupling structure in the three-body decays of the top and the anti-top quarks results in a large asymmetry between the charged leptons and the neutrinos. They do affect the charged leptons from the top identically to the ones from the anti-top, and therefore do not generate an asymmetry in the visible lepton decays (fig. 1). Concerning the leptons originating from the associated  $W$  boson, the ‘VA’ effects are present once the spin correlations of the associated  $W$  boson (denoted as  $W^{\text{pol}}$ ) are taken into account. In this case, as shown in fig. 2, the effects are different between the associated  $W^+$  and  $W^-$  and affect both the transverse momentum and pseudo-rapidity ratios.
- The most important source for the asymmetry is the top-quark pair polarization. Due to the associated  $W$ , these correlations are rather sizeable and significantly alter the shapes of the rapidities of the leptonic decays of the top quark as compared to

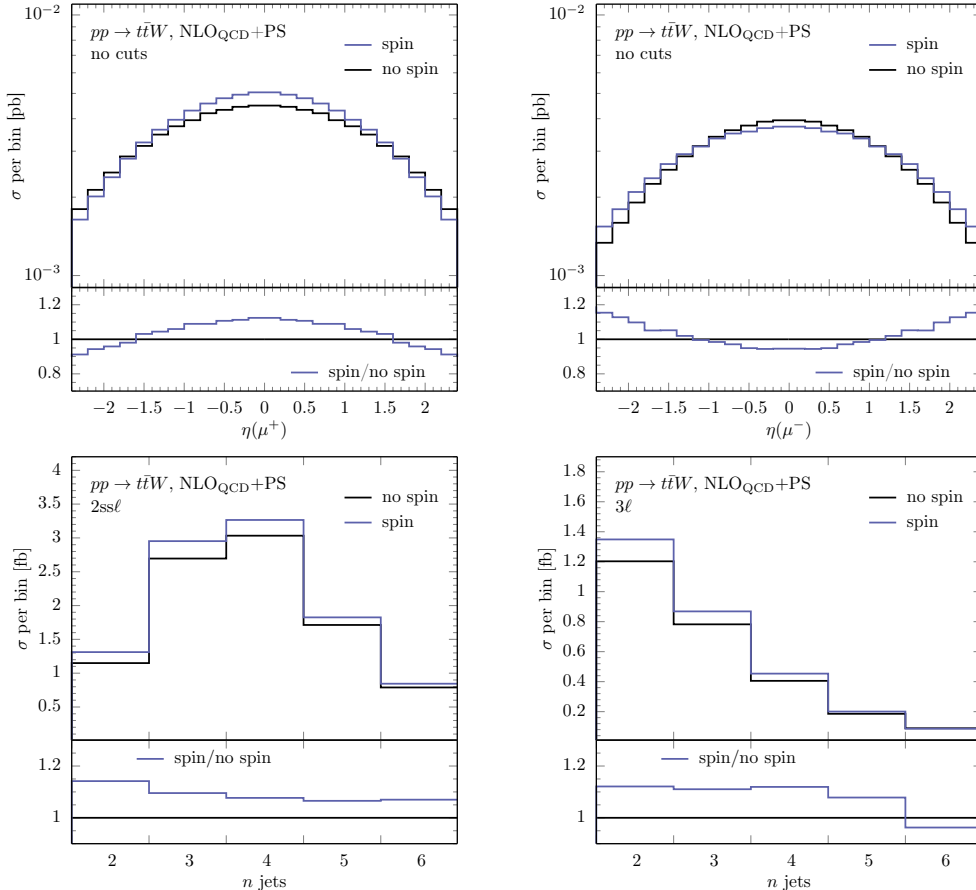


Figure 3: Spin correlation effects on lepton pseudo-rapidities and jet multiplicities. The muons in the upper plots are the leading in  $p_T$  regardless their origin.

the leptonic decays of the anti-top quark (denoted as  $t\bar{t}^{\text{pol}}$  in fig. 1). These effects result in a charge asymmetry of the leptons that reaches about -13–15% at the cross section level [8]. As shown in fig. 1 in the pseudo-rapidity ratio these effects are between  $\sim +20\%$  (central region) and  $\sim -40\%$  (peripheral region).

- The final source of asymmetry is due to the NLO electroweak corrections being of different size for  $t\bar{t}W^+$  and  $t\bar{t}W^-$  production. This is a negligible effect of  $\sim 0.5\%$  [6] and not considered in this work.

The consequences of these asymmetries on the  $t\bar{t}W$  background in the  $t\bar{t}H$  multi-lepton signatures are significant even at the cross section level. Since the largest of these effects are the spin correlations, we now compare the effect of these on the inclusive level as well as on the  $2\text{ssl}$  and  $3\ell$  signatures. As a first step, at the inclusive level (no cuts), we show in the two upper plots of fig. 3 that these effects are not altered by adopting the realistic setup described in section 2, i.e. including QED-shower, hadronisation, and underlying event. As one can see from figs. 1 and 2 and the upper two plots of fig. 3, the spin correlations allow more  $\ell^+$ 's than  $\ell^-$ 's within the selection criteria (eq. 2.3). This, in combination with the fact that there are more  $\ell^+$ 's produced than  $\ell^-$ 's due to the  $t\bar{t}W^+$  cross section being larger than the  $t\bar{t}W^-$  one by a factor of  $\sim 2$ , increases the fiducial cross section of  $t\bar{t}W$  production in both the  $2\text{ssl}$  and  $3\ell$  signatures. This can also be seen in the two lower plots of fig. 3, where we show the jet multiplicities with and without the spin-correlation effects for the  $2\text{ssl}$  and  $3\ell$  signatures in the left and right plots, respectively.

Jet multiplicity:	inclusive	0	1	2	3	4	5	6
no cuts	1.977(2)	2.88(4)	2.43(1)	2.218(7)	2.087(4)	2.003(3)	1.956(3)	1.916(3)
no cuts-no spin	1.977(1)	2.90(4)	2.45(1)	2.205(7)	2.087(5)	2.003(4)	1.956(3)	1.920(3)
2ssl	1.99(2)	-	-	2.30(3)	2.02(2)	1.96(2)	1.94(3)	1.84(4)
2ssl-no spin	1.84(1)			1.90(3)	1.84(2)	1.84(2)	1.84(3)	1.72(4)
3ℓ	1.88(2)	-	-	1.89(3)	1.92(4)	1.81(5)	1.83(8)	1.8(1)
3ℓ-no spin	1.84(2)			1.81(3)	1.82(4)	1.86(5)	1.90(8)	1.9(1)

Table 1: Charge ratio  $\sigma_{t\bar{t}W^+}/\sigma_{t\bar{t}W^-}$  in different signatures. The scale uncertainties can be taken to be correlated and are therefore of the order of the statistical error (in parantheses) and are not shown.

The increase in the cross section due to the spin correlations between the top and the anti-top is about 10% and slightly larger for the lower-multiplicity bins as compared to the higher ones.

Alternatively, the effects of the spin correlations can be presented in the value of the charge ratio  $\sigma_{t\bar{t}W^+}/\sigma_{t\bar{t}W^-}$  for the various signatures. This is shown in tab. 1. In this table we show the ratio for the total cross section and bin by bin for the jet multiplicity in both signatures. As a reference and in accordance with fig. 3, we also show the same ratio before any selections or cuts (no cuts) as well as before the spin-correlation effects (no spin) are taken into account. As expected, the inclusive result (before any selections or cuts) is not affected by the spin correlations. Without including the latter, in both signatures the charge ratio decreases from 1.977 to 1.84. This is mostly due to the decrease of the  $\eta(e^+)/\eta(e^-)$  ratio in the central pseudo-rapidity region due to the PDF effect, as shown in fig. 2. By including the spin-correlation effects the charge ratio in the 2ssl signature increases, and accidentally agrees within the uncertainties with the inclusive result. In the 3ℓ signature the ratio also increases, but less. This is due to the strong preference of the 2ssl signature to the positively charged lepton pair as shown in the pseudo-rapidity distributions of fig. 1 and which we will now elaborate on in more detail.

In the 2ssl signature it is more often that the anti-top (as compared to the top) decays hadronically within this signal region. This is because  $\sigma(t\bar{t}W^+) > \sigma(t\bar{t}W^-)$  and the (potential)  $\ell^+$  from top is more central than the (potential)  $\ell^-$  from the anti-top due to spin correlations. This results to a larger increase of the charge ratio due to spin correlations as compared to the 3ℓ signature, where all three massive particles need to decay (semi-)leptonically. Hence, for the 3ℓ signature also the more-forward  $\ell^-$  from the anti-top needs to be within the selection criteria, resulting in a smaller increase due to spin correlations than for the 2ssl signature. Besides this, also the ‘PDF’ affects the 2ssl signature differently from the 3ℓ one. In both these signatures the associated  $W$  boson decays leptonically and the ‘PDF’ effect described in section 3.1 affects them in the same way. This is not true for the top-quark pair decay products. In the 3ℓ signature both the top and anti-top quarks decay semi-leptonically, therefore no extra asymmetry is induced from ‘PDF’ effect. However in the case of 2ssl signature there is an extra asymmetry induced due to the fact that for the positively charged lepton pair both leptons will be on average harder and more forward (emerging from  $t\bar{t}W^+$ ) as compared to the negatively charged lepton pair (emerging from  $t\bar{t}W^-$ ). Even though this effect is opposite to the one

from the top-quark pair spin correlations, the latter is always dominant, resulting in a larger charge ratio for the  $2ss\ell$  as compared to the  $3\ell$  signatures.

Concerning the jet multiplicity, the charge ratio decreases at the highest jet multiplicities, where the shower effects become important. We have checked that these results do not change significantly once we add the  $\text{EW}_{\text{sub}}$  contributions to the NLO QCD, as we will explain in section 3.2. We have also verified that already without misidentifications or identification inefficiencies there is a large migration of events from the 3-lepton decay mode to the  $2ss\ell$  signature (which is included in our results). However this effect is expected to be enhanced in the experimental analyses and there will also be the inverse migration (2-lepton decay mode to  $3\ell$  signature). Therefore the results presented in fig. 3 and tab. 1 are expected to be sensitive to these effects and should be reconsidered with full detector simulation.

### 3.2 Subleading EW contributions

Having understood in section 3.1 the origin of the lepton asymmetries and their impact on the different final signatures we proceed to the discussion on the  $\text{EW}_{\text{sub}}$  contributions, as defined in equation 2.1. It is shown in ref. [11] and discussed in detail in ref. [5] that the

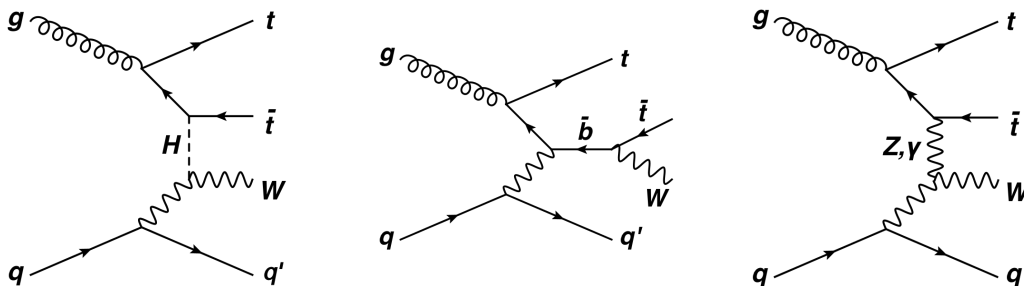


Figure 4: Dominant representative Feynman diagrams for the  $\text{EW}_{\text{sub}}$  contributions in the  $\alpha_s\alpha^3$  perturbative order.

$\sim 10\%$  the  $\text{EW}_{\text{sub}}$  contributions originate almost exclusively from the  $\alpha_s\alpha^3$  perturbative order (the  $\text{NLO}_3$  in the notation of ref. [5]). The dominant representative diagrams of this contribution are shown in fig. 4. These contributions are  $qg$  initiated with different structure w.r.t. the  $q\bar{q}$  initiated contributions that cause the large lepton asymmetries already at LO. Therefore the presence of the  $W$  boson does not result to the same spin correlations for the top pair decay products. This can be seen in the plots in fig. 5,

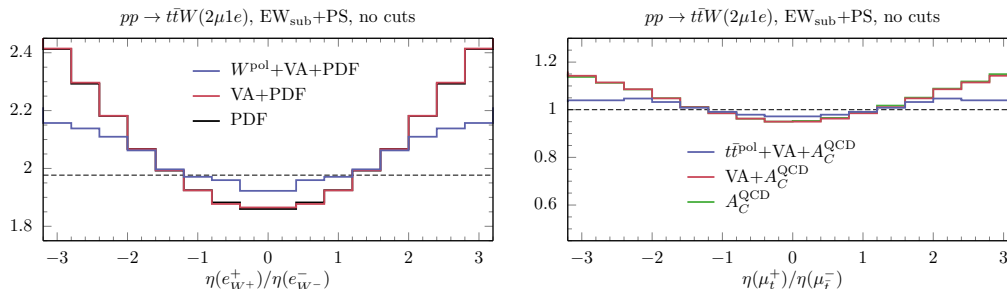


Figure 5: Origin of asymmetries in  $W$  associated (left) and top-quark pair (right) decay products for the  $\text{EW}_{\text{sub}}$  perturbative orders.



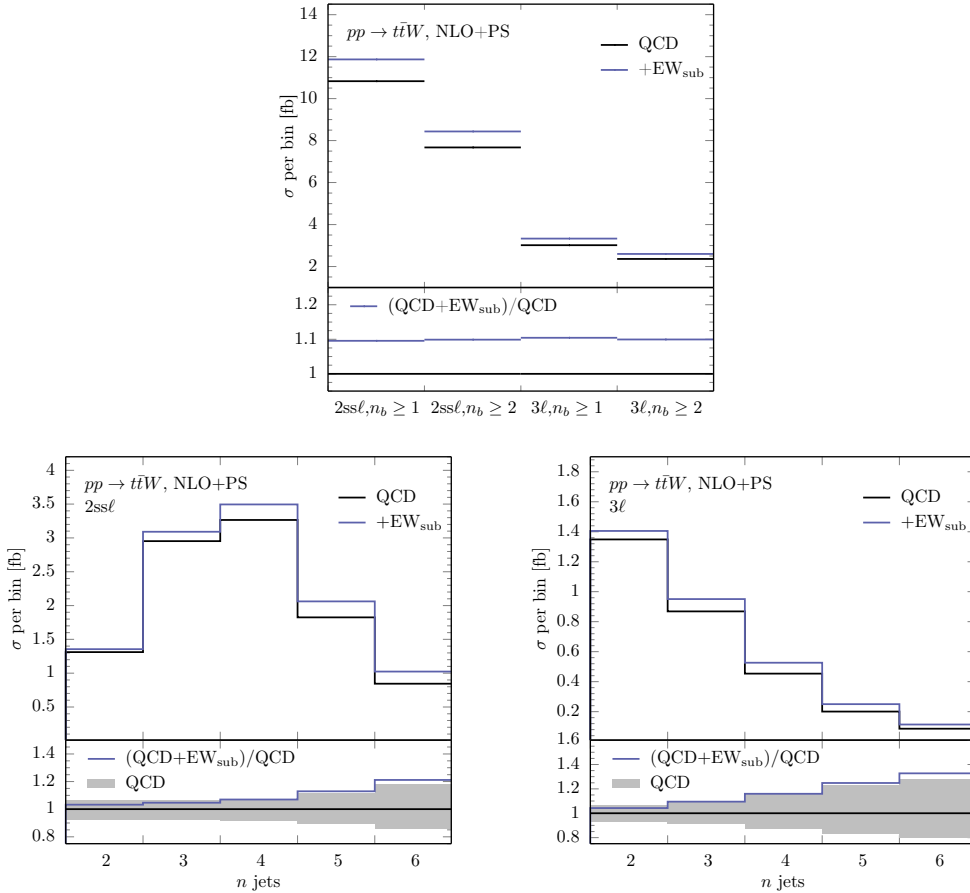


Figure 6: Effect of the  $\text{EW}_{\text{sub}}$  contributions on the cross section and the jet multiplicities for the  $2\text{ssl}$  and  $3\ell$  signatures.

for which we follow the same setup as for figs. 1 and 2. Regarding the associated  $W$  boson decay products (left plot) the contribution of the various effects is similar to the corresponding ones at NLO in QCD (lower left plot in fig. 2). However this is not the case for the top-quark pair decay products (right plot). Due to the aforementioned differences of these contributions, the large effect of the top-quark pair spin correlations (lower right plot in fig. 1) is not there. This last remark shows that the inclusion of the  $\text{EW}_{\text{sub}}$  contributions slightly flattens the asymmetries of the top-quark pair leptons. The overall effect is small, since the total contribution from the  $\text{EW}_{\text{sub}}$  is only  $\sim 10\%$ . As a result the charge ratio presented in tab. 1 is not altered within the given statistical MC errors by the inclusion of the  $\text{EW}_{\text{sub}}$  perturbative orders. In the next paragraph we explore the effect of the  $\text{EW}_{\text{sub}}$  contributions to the total cross section and the jet multiplicities within the selected signatures.

Starting from the NLO QCD production the inclusion of the EW perturbative orders up to now is done by applying a flat scaling factor 0.96 for the  $-4\%$  contribution of the  $\alpha_s^2\alpha^2$  perturbative order and a 1.09 for the contribution of the  $\text{EW}_{\text{sub}}$  contributions [3]. In the upper plot of fig. 6 we start by showing the effect of the latter on the cross sections for both the  $2\text{ssl}$  and  $3\ell$  signatures requiring at least one ( $n_b \geq 1$ ) or two ( $n_b \geq 2$ ) b-jets. As shown in the plot, in all the selected signatures there is a  $10\%$  effect of the  $\text{EW}_{\text{sub}}$  contributions in agreement with the aforementioned applied scaling factor. In the lower two plots of fig. 6 the jet multiplicities in the  $2\text{ssl}$  and  $3\ell$  are shown in the left and right plot, respectively. From these plots one can see that the effects from the  $\text{EW}_{\text{sub}}$  are not

flat. In particular, they have a rather small effect in the low jet-multiplicity bins, but are significantly larger in the higher jet-multiplicity bins. Hence, they behave opposite from the spin-correlation effects presented in the lower plots of fig. 3. In the lower insets, also the scale uncertainties (obtained in the usual way by taking the envelope of the  $3 \times 3 = 9$  point variation of the renormalisation and factorisation scales) in the  $t\bar{t}W$  production process are shown. The  $EW_{\text{sub}}$  are just at the edge of the scale uncertainty band<sup>2</sup>. The main reason for this behaviour at the differential level is the fact that the dominant topologies of the  $EW_{\text{sub}}$  contributions (fig. 4) have an extra parton. As a result, the peaks of the jet multiplicities (lower plots of fig. 3) are shifted to the right and furthermore the extra parton increases the sources of radiation.

## 4 Conclusions

In this work we discussed two non-negligible effects in  $t\bar{t}W$  production: spin correlations in the top-quark pair and the large, formally subleading EW corrections (mainly) induced by  $tW \rightarrow tW$  scattering. In the current experimental analyses the former is included, whereas the latter is simulated via a flat  $K$ -factor. Concerning the spin correlations we disentangled every source of asymmetry relevant to the final signatures. We further studied and presented, for the first time, the impact of the  $EW_{\text{sub}}$  contributions on the selected signatures within a realistic analysis setup. We have found that both effects enhance the  $t\bar{t}W$  background in the  $2s\ell$  and  $3\ell$  signal regions of  $t\bar{t}H$  production by approximately 10%. However, their effects are not flat in the phase-space. In particular, we considered the cross sections binned in jet multiplicity and found that the spin correlation effects enhance the low jet multiplicities more than high jet multiplicities, and the  $EW_{\text{sub}}$  inducing an opposite effect. However, since the induced differences in shapes are rather different, also the combined effect of spin correlations and  $EW_{\text{sub}}$  contributions is not flat in phase-space. Hence, we can conclude that both effects are important, and that both effects need to be included in the analysis in a differential manner. For the latter effect, this work shows, for the first time, that this can indeed be done: it is possible to use the default MC@NLO matching, as available in Madgraph5\_aMC@NLO, to include the large  $EW_{\text{sub}}$  contributions (which include  $tW \rightarrow tW$  scattering) within the standard event generation framework.

## Acknowledgments

This work is done in the context of and supported by the Swedish Research Council under contract number 2016-05996. IT would like to thank Rohin Narayan for the detailed discussions on the experimental analysis.

## References

- [1] M. Aaboud *et al.* [ATLAS Collaboration], “Measurement of the  $t\bar{t}Z$  and  $t\bar{t}W$  cross sections in proton-proton collisions at  $\sqrt{s} = 13$  TeV with the ATLAS detector,” Phys.

---

<sup>2</sup>One should keep in mind that, in particular for the larger multiplicities, there is also a significant uncertainty coming from the parton shower modeling, which we have not included here.

- Rev. D **99** (2019) no.7, 072009 doi:10.1103/PhysRevD.99.072009 [arXiv:1901.03584 [hep-ex]].
- [2] A. M. Sirunyan *et al.* [CMS Collaboration], “Measurement of the cross section for top quark pair production in association with a W or Z boson in proton-proton collisions at  $\sqrt{s} = 13$  TeV,” JHEP **1808** (2018) 011 doi:10.1007/JHEP08(2018)011 [arXiv:1711.02547 [hep-ex]].
- [3] The ATLAS collaboration, “Analysis of  $t\bar{t}H$  and  $t\bar{t}W$  production in multilepton final states with the ATLAS detector,” ATLAS-CONF-2019-045.
- [4] CMS Collaboration, “Search for Higgs boson production in association with top quarks in multilepton final states at  $\sqrt{s} = 13$  TeV,” CMS-PAS-HIG-17-004.
- [5] R. Frederix, D. Pagani and M. Zaro, “Large NLO corrections in  $t\bar{t}W^\pm$  and  $t\bar{t}t\bar{t}$  hadroproduction from supposedly subleading EW contributions,” JHEP **1802** (2018) 031 doi:10.1007/JHEP02(2018)031 [arXiv:1711.02116 [hep-ph]].
- [6] A. Broggio, A. Ferroglia, R. Frederix, D. Pagani, B. D. Pecjak and I. Tsinikos, “Top-quark pair hadroproduction in association with a heavy boson at NLO+NNLL including EW corrections,” JHEP **1908** (2019) 039 doi:10.1007/JHEP08(2019)039 [arXiv:1907.04343 [hep-ph]].
- [7] A. Kulesza, L. Motyka, D. Schwartzlinder, T. Stebel and V. Theeuwes, “Associated top quark pair production with a heavy boson: differential cross sections at NLO+NNLL accuracy,” arXiv:2001.03031 [hep-ph].
- [8] F. Maltoni, M. L. Mangano, I. Tsinikos and M. Zaro, “Top-quark charge asymmetry and polarization in  $t\bar{t}W^\pm$  production at the LHC,” Phys. Lett. B **736** (2014) 252 doi:10.1016/j.physletb.2014.07.033 [arXiv:1406.3262 [hep-ph]].
- [9] F. Maltoni, D. Pagani and I. Tsinikos, “Associated production of a top-quark pair with vector bosons at NLO in QCD: impact on  $t\bar{t}H$  searches at the LHC,” JHEP **1602** (2016) 113 doi:10.1007/JHEP02(2016)113 [arXiv:1507.05640 [hep-ph]].
- [10] J. Alwall *et al.*, “The automated computation of tree-level and next-to-leading order differential cross sections, and their matching to parton shower simulations,” JHEP **1407** (2014) 079 doi:10.1007/JHEP07(2014)079 [arXiv:1405.0301 [hep-ph]].
- [11] R. Frederix, S. Frixione, V. Hirschi, D. Pagani, H.-S. Shao and M. Zaro, “The automation of next-to-leading order electroweak calculations,” JHEP **1807** (2018) 185 doi:10.1007/JHEP07(2018)185 [arXiv:1804.10017 [hep-ph]].
- [12] P. Artoisenet, R. Frederix, O. Mattelaer and R. Rietkerk, “Automatic spin-entangled decays of heavy resonances in Monte Carlo simulations,” JHEP **1303** (2013) 015 doi:10.1007/JHEP03(2013)015 [arXiv:1212.3460 [hep-ph]].
- [13] T. Sjöstrand *et al.*, “An Introduction to PYTHIA 8.2,” Comput. Phys. Commun. **191** (2015) 159 doi:10.1016/j.cpc.2015.01.024 [arXiv:1410.3012 [hep-ph]].
- [14] S. Frixione and B. R. Webber, “Matching NLO QCD computations and parton shower simulations,” JHEP **0206** (2002) 029 doi:10.1088/1126-6708/2002/06/029 [hep-ph/0204244].

- [15] S. Frixione, P. Nason and B. R. Webber, “Matching NLO QCD and parton showers in heavy flavor production,” JHEP **0308** (2003) 007 doi:10.1088/1126-6708/2003/08/007 [hep-ph/0305252].
- [16] S. Frixione, V. Hirschi, D. Pagani, H.-S. Shao and M. Zaro, “Electroweak and QCD corrections to top-pair hadroproduction in association with heavy bosons,” JHEP **1506** (2015) 184 doi:10.1007/JHEP06(2015)184 [arXiv:1504.03446 [hep-ph]].
- [17] J. H. Kuhn and G. Rodrigo, “Charge asymmetries of top quarks at hadron colliders revisited,” JHEP **1201** (2012) 063 doi:10.1007/JHEP01(2012)063 [arXiv:1109.6830 [hep-ph]].
- [18] W. Hollik and D. Pagani, “The electroweak contribution to the top quark forward-backward asymmetry at the Tevatron,” Phys. Rev. D **84** (2011) 093003 doi:10.1103/PhysRevD.84.093003 [arXiv:1107.2606 [hep-ph]].
- [19] W. Bernreuther and Z. G. Si, “Top quark and leptonic charge asymmetries for the Tevatron and LHC,” Phys. Rev. D **86** (2012) 034026 doi:10.1103/PhysRevD.86.034026 [arXiv:1205.6580 [hep-ph]].
- [20] M. Czakon, P. Fiedler and A. Mitov, Phys. Rev. Lett. **115** (2015) no.5, 052001 doi:10.1103/PhysRevLett.115.052001 [arXiv:1411.3007 [hep-ph]].
- [21] M. Czakon, D. Heymes, A. Mitov, D. Pagani, I. Tsiniikos and M. Zaro, “Top-quark charge asymmetry at the LHC and Tevatron through NNLO QCD and NLO EW,” Phys. Rev. D **98** (2018) no.1, 014003 doi:10.1103/PhysRevD.98.014003 [arXiv:1711.03945 [hep-ph]].
- [22] T. Aaltonen *et al.* [CDF Collaboration], “Measurement of the top quark forward-backward production asymmetry and its dependence on event kinematic properties,” Phys. Rev. D **87** (2013) no.9, 092002 doi:10.1103/PhysRevD.87.092002 [arXiv:1211.1003 [hep-ex]].
- [23] T. Aaltonen *et al.* [CDF Collaboration], “Measurement of the Differential Cross Section  $d\sigma/d(\cos\theta_t)$  for Top-Quark Pair Production in  $p - \bar{p}$  Collisions at  $\sqrt{s} = 1.96$  TeV,” Phys. Rev. Lett. **111** (2013) no.18, 182002 doi:10.1103/PhysRevLett.111.182002 [arXiv:1306.2357 [hep-ex]].
- [24] V. M. Abazov *et al.* [D0 Collaboration], “Measurement of the Forward-Backward Asymmetry in Top Quark-Antiquark Production in  $p\bar{p}$  Collisions using the Lepton+Jets Channel,” Phys. Rev. D **90** (2014) 072011 doi:10.1103/PhysRevD.90.072011 [arXiv:1405.0421 [hep-ex]].
- [25] T. A. Aaltonen *et al.* [CDF and D0 Collaborations], “Combined Forward-Backward Asymmetry Measurements in Top-Antitop Quark Production at the Tevatron,” Phys. Rev. Lett. **120** (2018) no.4, 042001 doi:10.1103/PhysRevLett.120.042001 [arXiv:1709.04894 [hep-ex]].